Appl. Phys. B 80, 993–1006 (2005)
DOI: 10.1007/s00340-005-1833-2

Applied Physics B
Lasers and Optics

M. ÁLVAREZ[1]
F. AMAT-GUERRI[2]
A. COSTELA[1], ✉
I. GARCÍA-MORENO[1]
C. GÓMEZ[1]
M. LIRAS[2,3]
R. SASTRE[3]

# Linear and cross-linked polymeric solid-state dye lasers based on 8-substituted alkyl analogues of pyrromethene 567

[1] Instituto de Química Física 'Rocasolano', CSIC, Serrano 119, 28006 Madrid, Spain
[2] Instituto de Química Orgánica, CSIC, Juan de la Cierva 3, 28006 Madrid, Spain
[3] Instituto de Ciencia y Tecnología de Polímeros, CSIC, Juan de la Cierva 3, 28006 Madrid, Spain

**Received: 17 December 2004 / Revised version: 31 March 2005**

**ABSTRACT** The lasing properties of analogues of the commercial laser dye pyrromethene 567 (PM567) incorporated (dissolved or copolymerized) into polymeric matrices have been studied using both linear and cross-linked methyl methacrylate-based copolymers with different degrees of functionalization. All synthesized dyes have the chromophore core of PM567 but with an $\omega$-acyloxypolymethylene chain at position 8. In general, the new materials exhibited laser emission with higher efficiencies and much higher photostabilities than those containing the commercial dye PM567 under the same experimental conditions. Lasing efficiencies of up to 40% were obtained under transversal pumping at 534 nm. The highest photostabilities, with the laser output remaining stable or dropping by less than 15% after 100 000 pump pulses at the same position of the sample, were reached in cross-linked materials with dyes covalently linked to the polymeric chains. When the polymeric samples were incorporated into a grazing-incidence grating oscillator, narrow-line-width operation with tuning ranges of up to 40 nm was obtained. These results show that efficient and photostable solid-state dye lasers competitive with their liquid counterparts can be developed by adequate chemical modifications in the dye molecules, as well as by the selection of appropriate polymeric formulations.

**PACS** 42.55.Mv; 42.55.Rz; 42.70.Hj; 42.70.Jk

## 1 Introduction

The development of tunable solid-state dye lasers, in which an organic dye is incorporated into a suitable solid matrix, is a subject of considerable interest and research activity [1]. Such lasers exhibit well-recognized advantages over conventional liquid dye lasers as they avoid the problems of toxicity and flammability posed by the use of organic solvents, present a low-cost gain medium, and are compact and easy to operate and maintain. Organic polymers are attractive host media for laser dyes since they exhibit good chemical compatibility with organic dyes, as well as high optical homogeneity and control of medium polarity and viscoelasticity, in a way similar to conventional solvents. Their structure and chemical composition can be easily modified, which allows us to introduce controlled changes to optimize their properties when used in a particular application [1, 2].

The lasing performance of organic dyes is ultimately limited by their triplet–triplet (T–T) absorption over the lasing spectral region. The highly coloured dipyrromethene·$BF_2$ compounds are a family of laser dyes which exhibit high fluorescence quantum yields owing to their low losses due to T–T absorption at the fluorescence emission wavelengths [3–11]. These dyes have been shown to emit laser radiation efficiently both in liquid [4, 9, 11–13] and solid state [1, 14–23], with some of them outperforming the laser performance of the reference dye rhodamine 6G (Rh6G). However, when reviewing the spectroscopic and photochemical parameters of the dipyrromethene·$BF_2$ dyes, one concludes that these dyes are not yet the ultimate high-efficiency and photostable laser dyes because they are not stable enough for the required uses and are particularly sensitive to photoreactions with oxygen [14, 24]. Trying to improve the lasing performance of these dyes, recent studies have demonstrated that their photophysical and lasing properties depend on their molecular structure, and that adequate substituents in the molecular core can enhance the laser action [25–28].

Special attention has been paid to the dye 4,4-difluoro-1,3,5,7, 8-pentamethyl-2,6-diethyl-4-bora-3a,4a-diaza-*s*-indacene, commercially known as pyrromethene 567 (PM567, Fig. 1) because of the simplicity of its chemical structure and its good laser performance in both liquid and solid state [1, 29]. The photophysical behaviour and the photochemical stability of this dye can be modulated by changes in the substitution pattern of the tricyclic ring system. Over the last few years, we have studied the effect of different substituents at the position 8 of this molecule, while maintaining the four methyl groups in the 1, 3, 5, and 7 positions and the ethyl groups in the 2 and 6 positions [26, 28, 30–32]. In particular, we have synthesized a number of analogues of the dye PM567 where the methyl group at position 8 was replaced by a methacryloyloxypolymethylene or an acetoxypolymethylene

---

✉ Fax: +34-91-564-2431, E-mail: acostela@iqfr.csic.es

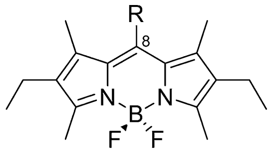

| | R | $n$ |
|---|---|---|
| PM567 | $-CH_3$ | |
| P$n$Ac | $-(CH_2)_nOCOCH_3$ | 1,3,5,10,15 |
| P$n$MA | $-(CH_2)_nOCOC(CH_3)=CH_2$ | 1,3,5,10,15 |

**FIGURE 1** Molecular structures of the dipyrromethene·$BF_2$ laser dye PM567 and the analogues studied herein

chain with $n$ methylenes, resulting in monomeric dyes P$n$MA and their model compounds P$n$Ac, respectively (Fig. 1) [31]. The presence of these substituents did not significantly modify the photophysics of the chromophore with regard to that of PM567, especially if the linear polymethylene chain has three or more methylene groups [30, 32]. These new dyes, when dissolved in a variety of organic solvents, lased more efficiently than PM567 and, under continuous UV irradiation, demonstrated improved photostability [26, 31]. When these modified dipyrromethene·$BF_2$ chromophores were either dissolved (P$n$Ac dyes) in poly(methyl methacrylate) (PMMA) or covalently bound (P$n$MA dyes) to the same polymer by copolymerization with methyl methacrylate (MMA), they lased more efficiently and with higher photostability than the parent dye PM567 incorporated into PMMA [28].

Our previous studies of polymeric solid-state dye lasers indicated that the best dye/host combination is specific for each dye molecule and that there is no universal polymeric matrix which can be used with all different dyes [1, 17]. Instead, the photophysical and photochemical properties of each particular dye require a proper adjustment of the polymer structure in order to obtain optical, thermal, and mechanodynamical properties of the matrix that optimize its laser action. The rigidity of the matrix, in particular, is of utmost importance in this regard. Thus, in the present work we explore the lasing properties of the former dipyrromethene·$BF_2$ dyes when incorporated into a number of linear and cross-linked copolymers. The actual composition of these materials was decided in the light of the information obtained in our previous studies of the lasing properties of PM567 dissolved in copolymers of MMA with different monomers [16, 17].

## 2 Experimental

### 2.1 *Materials*

The laser dye PM567 was from Exciton and used as received. The purity of the dye was found to be > 99%, as determined by spectroscopic and chromatographic methods. Details of the synthesis of the new dipyrromethene·$BF_2$ dyes have been reported elsewhere [31].

Linear copolymers were obtained by copolymerization of MMA with the monomers 2-hydroxyethyl methacrylate (HEMA), 2-hydroxyethyl acrylate (HEA), and 2,2,2-trifluoroethyl methacrylate (TFMA) (Fig. 2), selected to mimic the structures of liquid solvents where the new dyes operated with good performance [30]. Cross-linked materials were obtained by copolymerization of MMA with monomers with more than one polymerizable double bond per molecule, such as ethylene glycol dimethacrylate (EGDMA), trimethylolpropane trimethacrylate (TMPTMA), pentaerythritol triacrylate (PETA), and pentaerythritol tetraacrylate (PETRA) (Fig. 2). MMA (Merck) was washed three times with 10% w/v aqueous sodium hydroxide to remove the inhibitor and then two times with distilled water. HEMA (Alcolac) and HEA (Aldrich) were purified by standard methods immediately prior to use, and TFMA (Aldrich), EGDMA (Merck), TMPTMA (Solrac), PETA (Aldrich), and PETA (Aldrich) were used as received.

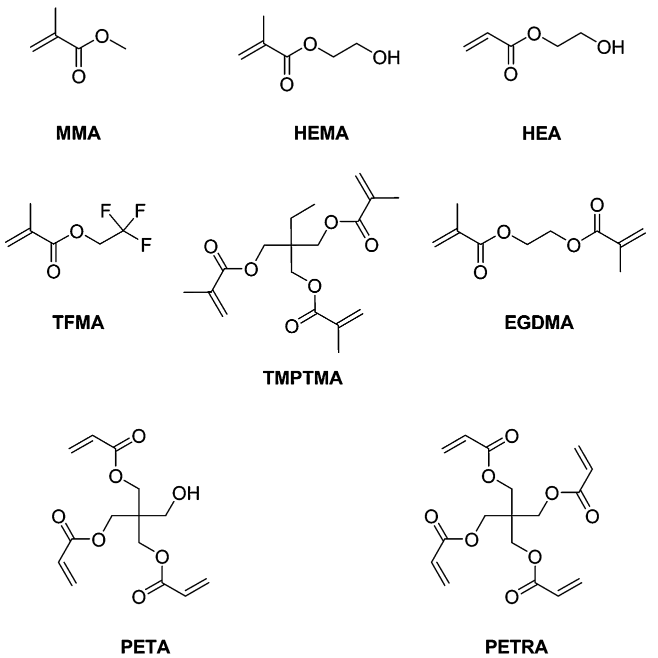

**FIGURE 2** Molecular structures of monomers: methyl methacrylate (MMA), 2-hydroxyethyl methacrylate (HEMA), 2-hydroxyethyl acrylate (HEA), 2,2,2-trifluoroethyl methacrylate (TFMA), trimethylolpropane trimethacrylate (TMPTMA), ethylene glycol dimethacrylate (EGDMA), pentaerythritol triacrylate (PETA), and pentaerythritol tetraacrylate (PETRA)

*2.1.1 Preparation of polymer dye samples.* Freshly purified monomers were used. An adequate amount of dye was dissolved in mixtures with different volume/volume ratios of MMA and other monomers, and the resulting mixtures were used for the preparation of the polymers, as described elsewhere [31].

Cylindrical-shaped samples, 10 mm in diameter and 10-mm high, were prepared from the unmolded polymeric rods. A cut was made parallel to the axis of the cylinder in order to obtain a lateral flat surface of ~ 4 × 10 $mm^2$. The ends of the rods and the lateral surface were prepared for lasing experiments by conventional grinding and polishing by hand to obtain reasonably flat surfaces.

A number of polymeric formulations with different plasticity and/or degree of cross linking were used as host materials for the dipyrromethene·$BF_2$ dyes. The basic monomer

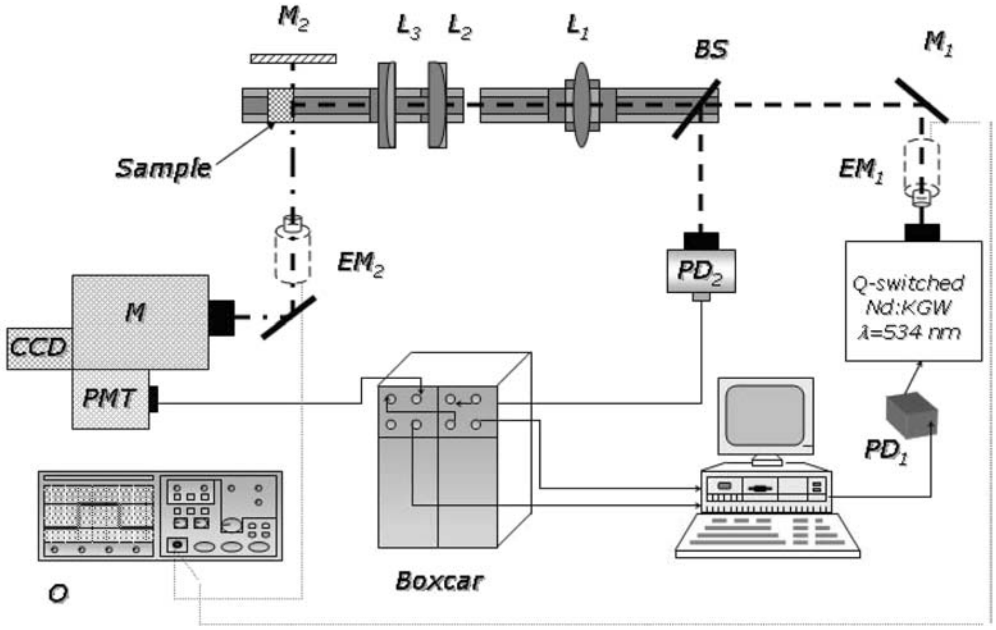

**FIGURE 3** Schematic of the laser system experimental setup. BS: beam splitter; CCD: CCD detector; EM: energy meters; $L_1$: spherical lens; $L_2$ and $L_3$: cylindrical lenses; M: monochromator; $M_1$ and $M_2$: aluminium flat mirrors; O: oscilloscope; PD: photodiodes; PMT: photomultiplier tube

of our polymers was MMA, because the homopolymer PMMA exhibits excellent optical transparency at the pump and lasing wavelengths, and high resistance to laser-radiation damage. Model dyes P*n*Ac were dissolved in the different matrices, rendering materials P*n*Ac/COP(MMA–monomer). Monomeric dyes P*n*MA were covalently linked to the polymeric chains, rendering the corresponding terpolymers TERP(P*n*MA–MMA–monomer).

## 2.2 *Methods*

A schematic diagram of the laser system is shown in Fig. 3. The air-equilibrated rods were transversely pumped at 534 nm with 5.5-mJ, 6-ns full width at half maximum (FWHM) pulses from a frequency-doubled *Q*-switched Nd:KGW laser (Monocrom STR-2+) at a repetition rate of 10 Hz. The exciting pulses were line focused on to the lateral flat surface of the solid samples by a combination of one spherical ($f = 50$ cm) and two cylindrical lenses ($f = -15$ cm and $+15$ cm, respectively) perpendicularly arranged. The first cylindrical lens widened the spherical cross section of the pump beam to illuminate the complete 1-cm length of the dye sample; then, the second cylindrical lens focused the pump beam on to the input surface of the solid sample to form a line of $0.3 \times 10\,\mathrm{mm}^2$. Typical pump fluence on the active medium was $180\,\mathrm{mJ/cm}^2$. The oscillation cavity consisted of a 90% reflectivity aluminium mirror and the end face of the sample as the output coupler, with a cavity length of 2 cm.

The dye and pump laser pulses were characterized with the following instruments: GenTec ED-100A and ED-200 energy meters, ITL TF fast-rise-time photodiode, Tektronix 2430 and TDS 3032 digital oscilloscopes, ARC SpectraPro-300i triple-grating monochromator and spectrograph, Acton Research SpectruMM:GS128B CCD detection system, and Hamamatsu R928 photomultiplier. Dye and pump laser signals were sampled with boxcars (Stanford Research, model 250). All the integrated signals were digitized and processed using a PC via a computer board DASH-8 interface [33]. The energy measurements were averaged over 16 shots. The estimated error of the energy measurements was 10%.

Narrow-line-width laser emission and tuning ranges of the dye-doped polymer samples were obtained by placing the samples in a home-made Shoshan-type oscillator [34], consisting of full-reflecting aluminium back and tuning mirrors and a 2400-lines/mm holographic grating in grazing incidence, with outcoupling via the grating zero order (Fig. 4). Wavelength tuning was accomplished by rotation of the tuning mirror. Tuning mirror and grating (both from Optometrics) were 5-cm wide and the angle of incidence on the grating was about 88.5°. Laser line width was measured with a Fabry–Perot etalon (IC Optical Systems) with a free spectral range of 15.9 GHz.

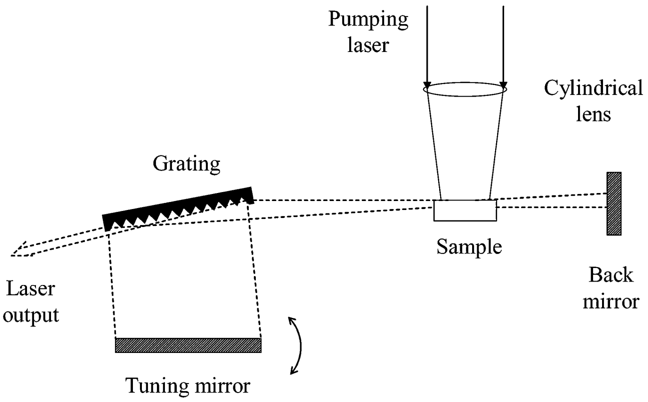

**FIGURE 4** Experimental arrangement of the narrow-line-width grating oscillator configured in the grazing-incidence geometry

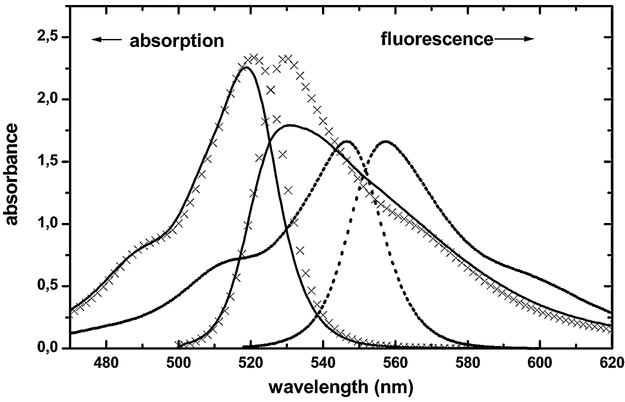

**FIGURE 5** Absorption and corrected fluorescence spectra of PM567 dissolved in PMMA (*full lines*), and of P10MA and P1MA copolymerized with MMA (*crosses and dots*, respectively)

Absorption and fluorescence spectra of the solid lasing samples were obtained from thin disks (0.2-mm thick, 5-mm diameter) cut out from the same samples used in the lasing experiments and measured, respectively, on a Shimadzu UV-267 FS spectrometer and on a Perkin Elmer LS-50B luminescence spectrometer.

## 3 Results and discussion

Broad-band laser emission with beam divergence of ≈ 5 mrad and pulse duration of ≈ 5 ns FWHM was obtained from all materials under study.

Our studies of the photophysical properties of P*n*Ac and P*n*MA dyes incorporated (dissolved or copolymerized, respectively) into PMMA matrices had demonstrated that the interaction between chromophore and substituent at position 8 was important in dyes with a short linking methylene chain ($n = 1$) but was negligible in those with longer polymethylene chains ($n \geq 3$) [32]. For dyes P1Ac and P1MA, this resulted in lower values of the fluorescence quantum yields and in an important red shift of absorption, fluorescence, and lasing emission spectra, as compared with P*n*Ac and P*n*MA ($n \geq 3$) dyes. Figure 5 shows the absorption and fluorescence spectra of the representative monomeric dyes P1MA and P10MA covalently bound to MMA, and of the parent dye PM567 dissolved in PMMA. In addition, the optimum concentration for efficient laser emission for dye P1Ac in liquid solution was found to be $0.45 \times 10^{-3}$ M, whereas for dyes P*n*Ac with longer polymethylene chains the highest lasing efficiencies were obtained at concentrations of about $1.5 \times 10^{-3}$ M [30]. Thus, for comparison purposes we first prepared and studied copolymers incorporating dissolved model dyes P*n*Ac ($n = 3, 5, 10$) and terpolymers formed with covalently bound monomeric dyes P*n*MA ($n = 3, 5, 10$), all of them with dye concentration $1.5 \times 10^{-3}$ M, and characterized their lasing properties.

### 3.1 *Laser operation in linear copolymers*

In our previous studies in liquid solution we had found improvements in the photophysical and lasing properties of the dipyrromethene·$BF_2$ dyes when the solvent was polar and protic and the solution diluted or moderately concentrated [30]. In solid samples, the polarity of the polymeric medium can be modulated by working with appropriate copolymers. Thus, we prepared copolymers of MMA with monomers functionalized with polar groups, such as HEMA and TFMA (Fig. 2). All linear copolymers and terpolymers were prepared with composition MMA:monomer 7:3 v/v, which had given rise to good photostability results when utilized with PM567 [16]. A schematic of the structure of the terpolymers resulting from the covalent linkage of monomeric dyes to linear copolymers is shown in Fig. 6.

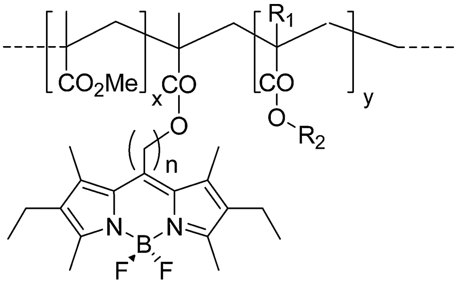

**FIGURE 6** Model structure of terpolymers formed from dyes P*n*MA and monofunctionalized monomers. TERP(P*n*MA–MMA–HEMA): $R_1 = CH_3$; $R_2 = CH_2OH$; TERP(P*n*MA–MMA–HEA): $R_1 = H$; $R_2 = CH_2OH$; TERP(P*n*MA–MMA–TFMA): $R_1 = CH_3$; $R_2 = CF_3$

The results obtained are summarized in Table 1. Previous results [28] obtained with the P*n*Ac and P*n*MA dyes dissolved in PMMA or copolymerized with MMA, respectively, are collected in Table 2.

From the data in Tables 1 and 2 it is seen that an increase in the polarity of the copolymer results in a slight hypsochromic shift of the laser emission, both in model and monomeric dyes. Lasing efficiencies in the range 24–40% were obtained in the linear copolymers and terpolymers (Table 1), depending on the dye and the matrix. These efficiencies are in general similar to or lower than those obtained with the same dyes dissolved in the homopolymer PMMA (dyes P*n*Ac) or copolymerized with MMA (dyes P*n*MA), which were in the range 34–41% (Table 2).

The lasing stability was studied by following the evolution of the laser emission with the number of pump pulses at 10-Hz repetition rate. Values of the laser output normalized to the initial lasing intensity after 30 000, 60 000, and, in selected cases, 100 000 pump pulses in the same position of the sample are collected in Tables 1 and 2. To facilitate comparison, we have represented graphically in Fig. 7 some of these data.

The stability of the materials consisting of terpolymers incorporating the monomeric dyes P*n*MA, where the chromophore is linked covalently to the polymeric chains, was always higher than that of the corresponding model dyes P*n*Ac simply dissolved in the same polymeric matrix (Table 1 and Fig. 7). This is the same behaviour previously observed when the dyes were incorporated into the homopolymer PMMA (Table 2 and Fig. 7). Nevertheless, the stabilities of both P*n*MA and P*n*Ac dyes in MMA–HEMA 7:3 matrices were always lower than in the homopolymer PMMA, except for dye P5Ac. When the polymeric material was the more polar

| Material | | $\lambda_{max}$ (nm) | $\Delta\lambda$ (nm) | Eff (%) | Laser output[b] | | |
|---|---|---|---|---|---|---|---|
| | | | | | $I_{30\,000}$ (%) | $I_{60\,000}$ (%) | $I_{100\,000}$ (%) |
| P3Ac/COP(MMA– | HEMA) | 565 | 5 | 30 | 52 | 36 | |
| | TFMA) | 563 | 5 | 24 | 78 | 49 | |
| TERP(P3MA–MMA– | HEMA) | 569 | 4 | 37 | 96 | 87 | |
| | TFMA) | 565 | 5 | 24 | 102 | 94 | |
| P5Ac/COP(MMA– | HEMA) | 565 | 6 | 39 | 87 | 83 | |
| | TFMA) | 565 | 6 | 39 | 78 | 57 | |
| TERP(P5MA–MMA– | HEMA) | 567 | 8 | 34 | 83 | 83 | 76 |
| | TFMA) | 565 | 9 | 38 | 90 | 80 | 70 |
| P10Ac/COP(MMA– | HEMA) | 562 | 5 | 30 | 17 | 9 | |
| | TFMA) | 561 | 8 | 40 | 72 | 50 | |
| TERP(P10MA–MMA– | HEMA) | 566 | 5 | 27 | 97 | 80 | |
| | TFMA) | 565 | 4 | 35 | 72 | 62 | 52 |

All materials with composition MMA:monomer 7:3 v/v. Dye concentration: $1.5 \times 10^{-3}$ M

[a] $\lambda_{max}$: peak of the laser emission; $\Delta\lambda$: FWHM of the laser emission; Eff: energy-conversion efficiency

[b] Intensity of the dye laser output after $n$ pump pulses in the same position of the sample referred to initial intensity $I_0$, $I_n(\%) = (I_n/I_0) \times 100$. Pump energy and repetition rate: 5.5 mJ and 10 Hz, respectively

**TABLE 1** Laser parameters[a] for model (P*n*Ac) and monomeric (P*n*MA) dyes in linear copolymers (COP) and terpolymers (TERP), respectively

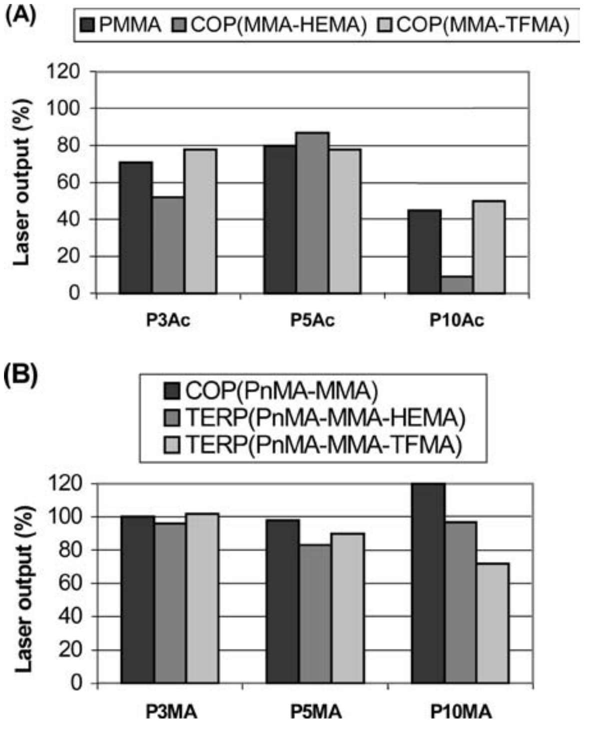

**FIGURE 7** Percent intensity, referred to initial intensity, of the laser output after 30 000 pump pulses in the same position of the sample: **A** model dyes P*n*Ac ($n = 3, 5, 10$) dissolved in linear copolymers; **B** monomeric dyes P*n*MA ($n = 3, 5, 10$) forming terpolymers with linear monomers. Results obtained in the homopolymer PMMA and in copolymers of monomeric dyes with MMA are also included for comparison. Dye concentration: $1.5 \times 10^{-3}$ M. Pump energy and repetition rate: 5.5 mJ/pulse and 10 Hz, respectively

mixture MMA–TFMA 7:3, the stability of the chromophore of the model dyes was about the same as, or higher than, in PMMA alone, whereas for the case of the same chromophore covalently bound to the same mixture (dyes P*n*MA) it was about the same as in PMMA, except for dye P10MA, where it was lower.

Trying to better assess the possible influence of the medium polarity on the stability of the modified dyes, we prepared terpolymers of P3MA dye with monomers MMA and TFMA in proportions 9:1 and 5:5 v/v, in addition to that in proportion 7:3. Material TERP[P3MA–(MMA–TFMA 9:1)] was less stable than TERP[PMA–(MMA–TFMA 7:3)], with the laser output dropping to 84% and 47% of the initial intensity after 30 000 and 60 000 pump pulses, respectively. Material TERP[P3MA–(MMA–TFMA 5:5)] exhibited a rather irregular behaviour with strong fluctuations: first the laser emission decreased to about 50% of the initial intensity after a few thousand shots, and after that it went up and down some more times. This behaviour is probably related to the drastic decrease in the glass-transition temperature of the polymeric material induced by the increased presence of TFMA. In fact, we were not able to prepare materials with an even higher proportion of TFMA because the excess plasticity of the resulting materials made them unfit for this application. These results seem to indicate that the composition MMA–TFMA 7:3 strikes the right balance between polarity and plasticity and optimizes the laser performance of the studied dyes in linear copolymers.

Attempts were also made to prepare matrices containing the acrylic monomer HEA because the formation of a methacrylic–acrylic copolymer increases the internal plasticity of the resulting polymeric material. Unfortunately, the presence of HEA decreases the glass-transition temperature of the material to values close to room temperature. As a result, after the usual thermal treatment, the obtained samples were rather soft, which makes the subsequent mechanization and proper polishing difficult. Even so, efficiencies of up to 35% were obtained with the modified dyes, but the laser emission decreased faster with the number of pump pulses due to the presence of residual monomers in these matrices, which causes degradation of the chromophores. When the material was subjected to an extended thermal treatment to reach the total polymerization of the residual double bonds, it resulted

| | | | | Laser output[a] | |
|---|---|---|---|---|---|
| Material | $\lambda_{max}$ (nm) | $\Delta\lambda$ (nm) | Eff (%) | $I_{30\,000}$ (%) | $I_{60\,000}$ (%) |
| P3Ac/PMMA | 569 | 4 | 36 | 71 | 50 |
| P5Ac/PMMA | 567 | 4 | 40 | 80 | (60)[b] |
| P10Ac/PMMA | 566 | 5 | 41 | 45 | |
| COP(P3MA–MMA) | 569 | 6 | 34 | 100 | 100 |
| COP(P5MA–MMA) | 568 | 5 | 36 | 98 | 75 |
| COP(P10MA–MMA) | 564 | 6 | 37 | 120 | 94 |

Dye concentration: $1.5 \times 10^{-3}$ M. Data from Ref. [28]

[a] As defined in Table 1

[b] After 50 000 pump pulses

**TABLE 2** Laser parameters[a] for model (P*n*Ac) and monomeric (P*n*MA) dyes dissolved in PMMA and copolymerized with MMA, respectively

in a much softer material, unfit for subsequent mechanization and polishing.

### 3.2 *Laser operation in cross-linked copolymers*

Both methacrylic (TMPTMA, EGDMA) and acrylic (PETA, PETRA) cross-linking monomers (Fig. 2), with different numbers of polymerizable groups per monomer molecule, were chosen for preparing three-dimensional cross-linked copolymers with MMA. EGDMA is a double functionalized monomer (two double bonds), TMPTMA and PETA are triple functionalized (three double bonds), and PETRA is quadruple functionalized (four double bonds). An important difference between the two triple functionalized cross-linking monomers is that PETA is acrylic, which, as indicated above, increases the plasticity of the resulting polymer or the mobility of the local segments between the cross-linking points of the resulting macromolecular net, and incorporates in its structure a hydroxy group, which should result in a more polar polymer. A schematic of the structure of the cross-linked copolymers tried in this work is shown in Fig. 8.

The lasing results obtained with the dyes P*n*Ac ($n = 3$, 5, 10) dissolved in the cross-linked copolymers, and with the terpolymers formed with the monomeric dyes P*n*MA ($n = 3$, 5, 10) covalently bounded to the polymeric chains are summarized in Table 3. Comparison with the results in Table 2 shows that whereas the laser emission wavelength is not significantly affected by cross linking, the lasing efficiencies in all the cross-linked materials are consistently lower than those obtained with the materials with the dyes dissolved in, or copolymerized with, the homopolymer. In general, the efficiencies obtained with the terpolymers are somewhat lower than those obtained with the model dyes dissolved in copolymers.

The photostability of the dyes under lasing conditions can be analysed from three different points of view: (i) influence of the covalent linkage of the chromophore to the polymer chains; (ii) influence of the length of the polymethylene chain, and (iii) influence of the degree of cross linking (i.e. influence of the polymeric free volume). Figure 9 shows the intensity of the laser output after 30 000 and 50 000 pump pulses in the same position of the sample, at 10-Hz repetition rate, for model dyes dissolved in cross-linked copolymers (materials P*n*Ac/COP(MMA–cross-linking monomer), $n = 3, 5, 10$) and for terpolymers with the monomeric dyes covalently bound to the polymeric chains (materials TERP(P*n*MA–MMA–cross-linking monomer), $n = 3$, 5, 10), in all cases with 95:5 v/v MMA–cross-linking monomer composition. Data for the same dyes incorporated into homopolymer PMMA (Table 2) are also included in Fig. 9 for comparison.

It can be appreciated from Fig. 9 that, as in the case of linear matrices, in cross-linked materials the photostability of monomeric dyes linked covalently to the polymeric chains is always higher than that of the corresponding model dyes dissolved in the copolymers. In addition, there is always at least one cross-linked composition where the P*n*MA dyes exhibit a photostability higher than the highest obtained with the same dye terpolymerized with linear copolymers (Tables 1 and 3, Figs. 7 and 9) and higher than those obtained in copolymers of the monomeric dyes with MMA (Tables 2 and 3, Fig. 9).

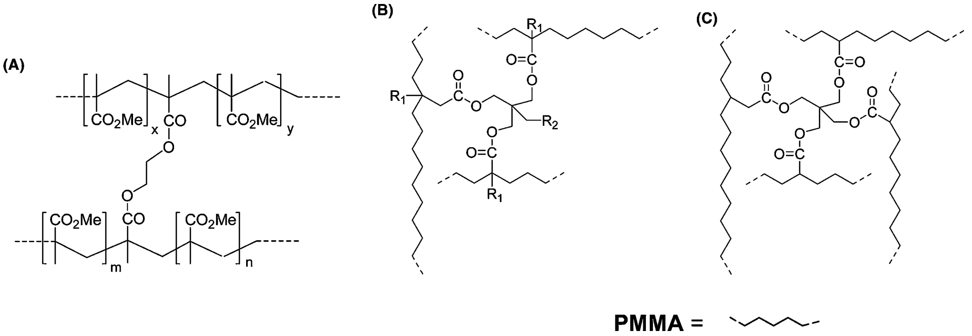

**FIGURE 8** Model structure of copolymers of MMA with cross-linked monomers: **A** COP(MMA–EGDMA); **B** COP(MMA–TMPTMA) ($R_1 = R_2 = CH_3$) and COP(MMA–PETA) ($R_1 = H$; $R_2 = OH$); and **C** COP(MMA–PETRA)

| Material | | $\lambda_{max}$ (nm) | $\Delta\lambda$ (nm) | Eff (%) | Laser output[a] | | | |
|---|---|---|---|---|---|---|---|---|
| | | | | | $I_{30\,000}$ (%) | $I_{50\,000}$ (%) | $I_{60\,000}$ (%) | $I_{100\,000}$ (%) |
| P3Ac/COP(MMA– | EGDMA) | 565 | 5 | 22 | 5 | | | |
| | TMPTMA) | 565 | 7 | 34 | 76 | 51 | | |
| | PETA) | 563 | 5 | 32 | 78 | 82 | 57 | |
| | PETRA) | 563 | 6 | 23 | 43 | 26 | 18 | |
| TERP(P3MA–MMA– | EGDMA) | 568 | 5 | 23 | 42 | 47 | 31 | 28 |
| | TMPTMA) | 565 | 5 | 28 | 105 | 111 | 112 | 133 |
| | PETA) | 567 | 5 | 33 | 72 | 75 | 59 | 70 |
| | PETRA) | 565 | 5 | 31 | 114 | 65 | 53 | |
| P5Ac/COP(MMA– | EGDMA) | 570 | 5 | 38 | 38 | 41 | | |
| | TMPTMA) | 566 | 4 | 32 | 85 | 78 | 77 | |
| | PETA) | 563 | 6 | 38 | 76 | 72 | 76 | |
| | PETRA) | 567 | 7 | 35 | 64 | 53 | | |
| TERP(P5MA–MMA– | EGDMA) | 565 | 5 | 29 | 62 | 48 | 32 | 60 |
| | TMPTMA) | 566 | 7 | 33 | 92 | 88 | 88 | 70 |
| | PETA) | 562 | 5 | 23 | 92 | 87 | 87 | |
| | PETRA) | 568 | 14 | 19 | 112 | 109 | 95 | 88[b] |
| P10Ac/COP(MMA– | EGDMA) | 562 | 5 | 38 | 66 | 48 | 40 | |
| | TMPTMA) | 561 | 10 | 33 | 72 | 49 | 47 | |
| | PETA) | 563 | 4 | 30 | 91 | 78 | 71 | |
| | PETRA) | 563 | 10 | 34 | 83 | 90 | 87 | |
| TERP(P10MA–MMA– | EGDMA) | 563 | 4 | 22 | 98 | 85 | 78 | |
| | TMPTMA) | 563 | 8 | 23 | 67 | 53 | 43 | 34 |
| | PETA) | 563 | 5 | 28 | 111 | 100 | 101 | |
| | PETRA) | 562 | 9 | 24 | 96 | 96 | 94 | 74 |

All materials with composition MMA–monomer 95:5 v/v. Dye concentration: $1.5 \times 10^{-3}$ M

[a] As defined in Table 1

[b] After 95 000 pump pulses

**TABLE 3** Laser parameters[a] for model (P*n*Ac) and monomeric (P*n*MA) dyes in cross-linked copolymers (COP) and terpolymers (TERP), respectively

To analyse the influence of the polymeric free volume on the photostability of the modified dyes, we have compared the behaviour of the dyes in matrices containing cross-linking monomers with two, three, or four polymerizable double bonds (EGDMA, TMPTMA, and PETRA, respectively). Laser emission from matrices containing the more polar monomer PETA will be analysed later. A higher number of polymerizable double bonds means a higher degree of cross linking and, thus, a smaller polymeric free volume. This relationship between cross-linking degree and polymeric free volume can be checked indirectly by determining the density of matrices prepared with increasing amounts of a given cross-linking monomer. In the second column of Table 4 are collected the densities, determined by a gravimetric method, of matrices composed of monomer dye P10MA covalently bound to monomers MMA and PETRA in ratios 98:2, 95:5, 90:10, and 80:20. As expected, the densities of the matrices increase with the amount of the cross-linking monomer PETRA, indicating a progressive decrease of the free volume.

The pattern of photostability behaviour of the dyes as a function of the material's degree of cross linking seems to be somewhat related to the length of the 8-chain in the dye molecules. In materials with dyes P3Ac (dissolved) and P3MA (covalently bound), the photostability first increases with the degree of cross linking until reaching a maximum in materials containing the triple functionalized monomer TMPTMA (Fig. 9A). Further increases in the degree of cross linking result in a decrease of photostability. Model dye P5Ac follows the same pattern, but in the materials with the covalently bound monomer dye P5MA the photostability

| Material | MMA–PETRA (v/v) | Density (g/cm$^3$) | $\lambda_{max}$ (nm) | Eff (%) | Laser output[a] | | |
|---|---|---|---|---|---|---|---|
| | | | | | $I_{30\,000}$ (%) | $I_{60\,000}$ (%) | $I_{100\,000}$ (%) |
| TERP(P10MA–MMA–PETRA) | 98:2 | 1.183 | 562 | 21 | 56 | 77 | 69 |
| | 95:5 | 1.186 | 562 | 24 | 96 | 94 | 74 |
| | 90:10 | 1.194 | 563 | 24 | 61 | 25 | |
| | 80:20 | 1.209 | 562 | 21 | 66 | 33 | 20 |

Dye concentration: $1.5 \times 10^{-3}$ M

[a] As defined in Table 1

**TABLE 4** Laser parameters[a] for terpolymers of monomer dye P10MA with monomers MMA and PETRA in different v/v ratios

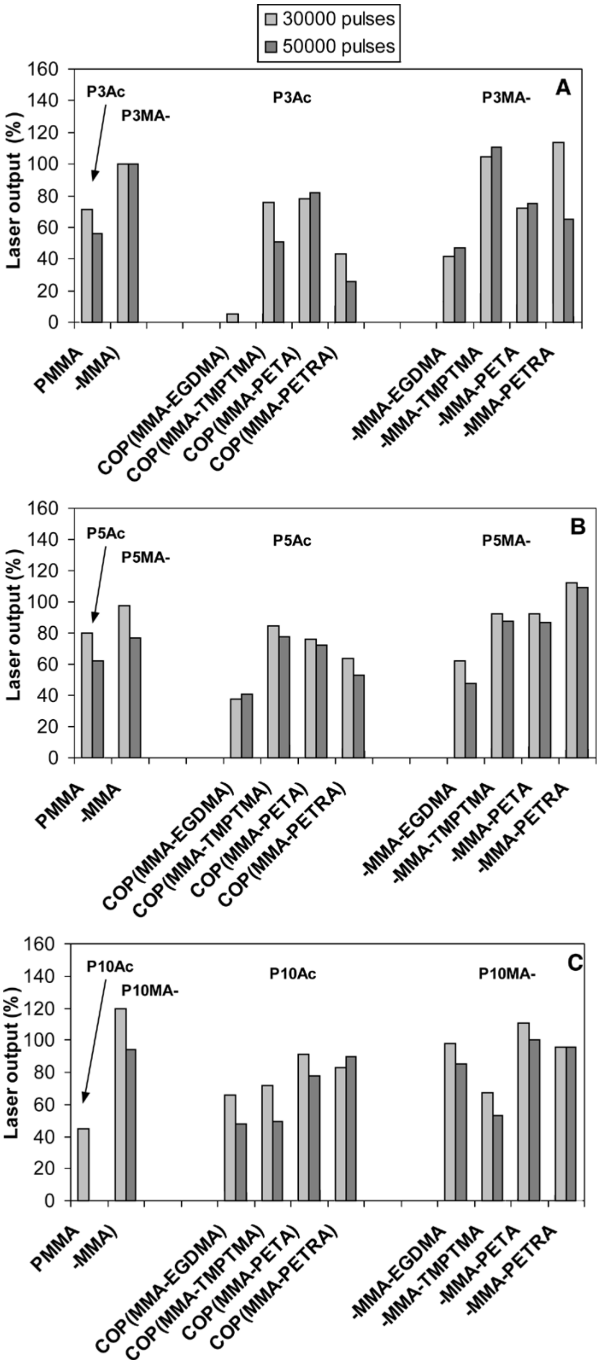

**FIGURE 9** Percent intensity, referred to initial intensity, of the laser output from **A** dyes P3Ac and P3MA, **B** dyes P5Ac and P5MA, and **C** dyes P10Ac and P10MA incorporated (dissolved or terpolymerized, respectively) into cross-linked copolymers after 30 000 and 50 000 pump pulses in the same position of the sample. Results obtained in the homopolymer PMMA are also included for comparison. Dye concentration: $1.5 \times 10^{-3}$ M. MMA–monomer composition: 95:5 v/v. Pump energy and repetition rate: 5.5 mJ/pulse and 10 Hz, respectively

keeps increasing with the degree of cross linking and the highest photostability is obtained in the matrix containing the monomer PETRA, with four polymerizable double bonds (Fig. 9B). This last behaviour is also observed in materials with dyes P10Ac (dissolved) and P10MA (covalently bound) (Fig. 9C), although with the anomalous behaviour of the material with dye P10MA, where the photostability first decreases and then increases with the degree of cross linking, with a minimum value in the matrix MMA–TMPTMA 95:5. This anomaly will be analysed later. It seems that the degree of cross linking which maximizes the photostability has not yet been reached in the dyes with the longer chain at position 8.

The general tendencies discussed above point to the importance of the proper adjustment of the rigidity of the polymeric matrix in the laser performance of lasing dyes. As the degree of cross linking increases, the available free volume in the polymer decreases. It seems that, in general, this factor controls the photodegradation processes of dyes dissolved in polymeric matrices at the concentration needed for laser operation in transversal pumping schemes. For a certain cross-linking degree, the free volume available within the polymeric matrix will be completely occupied by the dye. Increasing the degree of cross linking beyond this point will result in the dye molecules being partially excluded from the shrinking free volume, and formation of dimers and higher aggregates, with their deleterious effect on laser operation, will be forced. In the present case, the results obtained indicate that the cross-linking monomer must have at least three reactive double bonds in order to obtain a material with high photostability.

At first sight, the above argument seems to be contradictory with the observed behaviour of the modified dyes. The model (P*n*Ac) and monomeric (P*n*MA) dyes, with $n = 3$, 5, and 10, differ in the length of their chains at position 8, and it can be supposed that the size of the molecule would increase as the 8-chain becomes larger, provided that the chain was fully extended, as happens in liquid solution. According to the argument in the above paragraph, the lower the size of the molecule, the smaller the free volume which optimizes the stability of the laser emission. Thus, the dissolved P3Ac and covalently bound P3MA dyes should exhibit their highest photostability in matrices with higher cross-linking degree than the ones which stabilize the P5Ac, P5MA, P10Ac, and P10MA dyes, in contradiction with the experimental results. To understand the observed behaviour of the modified dyes, it should be taken into account that the length of the chain at position 8 will determine its conformation. The polymethylene chain ends with an ester group which cannot be placed near the indacene ring due to the electrostatic repulsion between the oxygen atoms of the ester group and the $\pi$ cloud of the aromatic rings, but there is no restriction in the movement of the bonds between methylenes. Thus, we can hypothesize that, taking into account the bond lengths, it seems that the chain at position 8 in dyes P3Ac and P3MA can be more extended than in dyes P5Ac, P5MA, P10Ac, and P10MA, with a larger number of methylenes, where the 8-chain can be folded, even surrounding the indacene core, so that the final volume occupied by the molecule would be smaller than that of the P3Ac and P3MA dyes.

To gain more insight into the dependence of the laser emission on the ratio of monomers in the solid matrix, we prepared terpolymers of the monomer dye P10MA with three different MMA–PETRA ratios, 98:2, 90:10, and 80:20, and evaluated the lasing properties of the resulting materials. The results obtained are collected in Table 4, where the results previously obtained for these materials with composition MMA–PETRA 95:5 and already tabulated in Table 3 are also included to facilitate comparison. It is seen that both the lasing efficiency and

| Material | | $\lambda_{max}$ (nm) | $\Delta\lambda$ (nm) | Eff (%) | Laser output[a] | | | |
|---|---|---|---|---|---|---|---|---|
| | | | | | $I_{30\,000}$ (%) | $I_{50\,000}$ (%) | $I_{60\,000}$ (%) | $I_{100\,000}$ (%) |
| P10Ac/COP(MMA– | TMPTMA 99:1) | 564 | 9 | 34 | 76 | 68 | 59 | |
| | TMPTMA 95:5) | 561 | 10 | 33 | 72 | 49 | 47 | |
| TERP(P10MA–MMA– | TMPTMA 99:1) | 564 | 8 | 27 | 84 | 94 | 90 | 86 |
| | TMPTMA 95:5) | 563 | 8 | 23 | 67 | 53 | 43 | 34 |

Dye concentration: $1.5 \times 10^{-3}$ M
[a]As defined in Table 1

**TABLE 5** Laser parameters[a] for P10 dyes in cross-linked copolymers (COP) and terpolymers (TERP) containing monomers MMA and TMPTMA in 99:1 and 95:5 v/v ratios

the photostability first increase with the amount of PETRA, and then decrease for proportions of PETRA higher than 5% in volume. This dependence is the same as that observed with the dye PM567 when incorporated into copolymers of MMA with PETRA [17].

As pointed out before, the behaviour of the material with the monomer dye P10MA covalently bound to MMA–TMPTMA 95:5 deviates from the trend followed by all the other dyes when incorporated into the same polymeric material (Fig. 9). When the reference dye PM567 was dissolved in cross-linked copolymers, the composition MMA–TMPTMA 99:1 had resulted in a much higher photostability than the 95:5 one [17]. Thus, we prepared samples of model and monomeric dyes with the composition MMA–TMPTMA 99:1, and studied their lasing behaviour. It was found that the photostability behaviour of dyes P*n*Ac and P*n*MA ($n = 3, 5, 10$) in the two MMA–TMPTMA compositions depended on the length of the 8-chain: shorter-chain P3 dyes were less photostable in composition 99:1 than in composition 95:5; model dye P5Ac worked slightly better in composition 99:1, and the stability of the covalently bound monomer dye P5MA was clearly higher with composition 95:5. The results obtained with dyes P10Ac and P10MA are collected in Table 5. To facilitate comparison, the results obtained with composition MMA–TMPTMA 95:5, already tabulated in Table 3, have also been included in Table 5. It is seen that both dissolved model dyes P10Ac and covalently bound monomer dyes P10MA worked better in the composition MMA–TMPTMA 99:1 than in the 95:5 one. If these results are incorporated into Fig. 9C, the anomaly in the behaviour of the photostability of both P10 dyes as the cross-linking degree is increased disappears, and the photostability becomes intermediate between that in MMA–EGDMA and that in MMA–PETRA.

The complexity of the mechanisms involved in the laser action of the studied materials and the specificity of the dye/matrix combination that optimizes the laser operation can be appreciated when comparing the results obtained with two different triple functionalized monomers, one methacrylic (TMPTMA) and the other acrylic (PETA). When monomers TMPTMA and PETA are copolymerized with MMA in the same v/v ratio (MMA:monomer 95:5), they determine the same cross-linking degree, but the different chemical composition of the matrix results in a drastic effect on the lasing photostability (Table 3 and Fig. 9). This is clearly illustrated by the behaviour of the monomeric dyes. With dye P3MA the monomer TMPTMA stabilizes the laser action over 100 000 pump pulses, whereas the presence of monomer PETA in the matrix results in a 30% decrease in the intensity of the laser emission after 100 000 pump pulses. When the length of the chain at position 8 of the dye increases, this behaviour reverses, and in the polymer with dye P10MA the photostability of the laser emission is higher with monomer PETA in the matrix.

### 3.3 *Laser operation in materials incorporating dissolved model dyes P1Ac and covalently bound polymeric dyes P1MA. Influence of dye concentration*

As indicated above, the optimum concentration for laser emission of P1Ac in liquid solution was significantly lower than those for model dyes with longer polymethylenic chains. Thus, for the sake of completeness of our study, we also prepared solid samples incorporating P1Ac at two different concentrations: $0.45 \times 10^{-3}$ M, which is the concentration that optimizes the efficiency of the laser emission for this dye, and $1.5 \times 10^{-3}$ M, which was the standard concentration utilized with dyes P*n*Ac ($n = 3, 5, 10$). Table 6 collects the results obtained with dye P1Ac dissolved in linear and cross-linked copolymers and in the homopolymer PMMA. The influence on the chromophore core of the acetoxymethyl group in position 8 of the dye P1Ac produces a large red shift in its fluorescence spectrum (Fig. 5) and a red shift of the peak wavelength of the laser emission of up to 25 nm, with respect to the longer polymethylenic chain dyes. In addition, at the lower dye concentration there can be appreciated an important hypsochromic shift of the laser emission in the linear copolymers as compared with the cross-linked structures. This shift is minimal or non-existent at the higher dye concentration, probably reflecting a complex balance between increased polarity of the polymeric medium and increased concentration of the dye. In general, the line width of the laser emission widens when P1Ac is dissolved in the copolymers, as compared with that of the same dye dissolved in the homopolymer PMMA.

For both linear and cross-linked monomers the increase of dye concentration by a factor of three results in a slight decrease in lasing efficiency, but in significant increases in laser photostability (except for the copolymer containing HEMA, where there is only a slight increase in the long-term photostability) (Table 6). As indicated above, a higher concentration compensates the photodegradation of the dye molecules and results in an apparent increase in photostability. Thus, in practice, a compromise should be reached between the conflicting requirements for efficiency and photostability, using a concentration which improves

| Material | | $c/10^{-3}$ (M) | $\lambda_{max}$ (nm) | Eff (%) | $\Delta\lambda$ (nm) | Laser output[a]<br>$I_{30\,000}$ (%) | <br>$I_{60\,000}$ (%) |
|---|---|---|---|---|---|---|---|
| P1Ac/PMMA[b] | | 0.45 | 591 | 5 | 31 | 16 | |
| P1Ac/COP(MMA–HEMA) | | 0.45 | 577 | 9 | 26 | 86 | 56 |
| P1Ac/COP(MMA–TFMA) | | 0.45 | 579 | 17 | 32 | 42 | 44 |
| P1Ac/COP(MMA– | EGDMA) | 0.45 | 583 | 14 | 25 | 69 | 24[c] |
| | TMPTMA) | 0.45 | 591 | 13 | 32 | 0[d] | |
| | PETA) | 0.45 | 591 | 10 | 30 | 40 | 0[c] |
| P1Ac/PMMA[e] | | 1.5 | 591 | 5 | 28 | 106 | 58 |
| P1Ac/COP(MMA–HEMA) | | 1.5 | 591 | 9 | 23 | 81 | 59 |
| P1Ac/COP(MMA–TFMA) | | 1.5 | 589 | 11 | 24 | 89 | 64 |
| P1Ac/COP(MMA– | EGDMA) | 1.5 | 592 | 11 | 26 | 67 | 32 |
| | TMPTMA) | 1.5 | 594 | 9 | 25 | 60 | 48 |
| | PETA) | 1.5 | 592 | 7 | 16 | 94 | 77 |
| | PETRA) | 1.5 | 591 | 12 | 27 | 90 | 107 |
| TERP(P1MA–MMA– | TMPTMA) | 1.5 | 589 | 10 | 24 | 87 | 35 |
| | PETRA) | 1.5 | 592 | 10 | 20 | 45 | 42 |

Results obtained with dye P1Ac dissolved in homopolymer PMMA and with monomer dye P1MA forming part of selected terpolymers are also included for comparison

[a] As defined in Table 1; $c$: dye concentration

[b] Data from Ref. [32]

[c] After 50 000 pump pulses

[d] After 17 000 pump pulses

[e] Data from Ref. [28]

**TABLE 6** Laser parameters[a] for two different concentrations of the model dye P1Ac dissolved in linear and cross-linked copolymers (COP) with compositions MMA–monomer 7:3 and 95:5 v/v, respectively

photostability while decreasing efficiency only moderately. In the present case, the best election corresponds to the most cross-linked matrix (composition MMA–PETRA), where no sign of degradation is observed in the laser output after 60 000 pump pulses while maintaining a reasonable lasing efficiency.

The main difference observed in the behaviour of dye P1Ac dissolved in cross-linked matrices with respect to that observed when this dye was dissolved in linear copolymers is that the peak wavelength of the laser emission is neither affected by the dye concentration nor by the degree of cross linking (except for the copolymer with EGDMA at the lower dye concentration).

At the beginning of Sect. 3 it was indicated that in dyes with the shorter linking chain (dyes P1Ac and P1MA) the substituent at position 8 influences the chromophore, affecting the properties of the laser operation. To assess the effect of further increasing the rigidity of the material in this case, we prepared terpolymers of monomer dye P1MA $1.5 \times 10^{-3}$ M with MMA and triple and quadruple functionalized monomers TMPTMA and PETRA, respectively (proportion MMA:cross-linking monomer: 95:5 v/v). Lasing results obtained with these terpolymers are included in Table 6. Lasing efficiencies were 24% and 20% for TERP(P1MA–MMA–TMPTMA) and TERP(P1MA–MMA–PETRA), respectively, showing the same tendency found in dyes with a longer 8-chain, where the efficiencies obtained with the covalently bound monomeric dyes in the cross-linked materials were in general lower than those obtained with the model dyes. Regarding photostability, it is seen that the terpolymer containing the triple functionalized monomer TMPTMA exhibits a stability somewhat lower than that of the model dye dissolved in the copolymer MMA–TMPTMA, whereas the stability of monomer dye in the material with quadruple functionalized PETRA is much lower than that of the model dye dissolved in the corresponding material. This seems to be a situation where the optimum degree of cross linking has been exceeded, resulting in a worsening in lasing performance, as discussed above.

### 3.4 *Evolution of the laser spectrum with the number of pump pulses*

When the spectrum of the laser emission of the modified dipyrromethene·$BF_2$ dyes was recorded as a function of the number of pump pulses, a slight displacement to the blue of the laser emission peak was usually observed. This is to be expected due to the decrease in the local concentration of the dye as the dye molecules are degraded. What was unexpected was the appearance of a new feature in the spectra: in addition to the initial peak of the laser emission, a second peak, placed at 10–12 nm to the blue with respect to the initial main peak, does appear (Fig. 10). This second peak increases with the number of pump pulses at the same time as the initial main peak decreases. It does appear earlier, and is more important, in model dyes than in monomeric dyes, as is illustrated in the example shown in Fig. 10.

A detailed assessment of the spectral evolution of the laser emission with the number of pump pulses was carried out with monomer dye P10MA incorporated into matrices with increased amounts of monomer PETRA considered above (Table 4). The results obtained are displayed in Fig. 11. It is seen that in the matrix with the lowest ratio of PETRA (Fig. 11A) the second peak remains much lower than the initial peak even after 100 000 pump pulses in the same position of

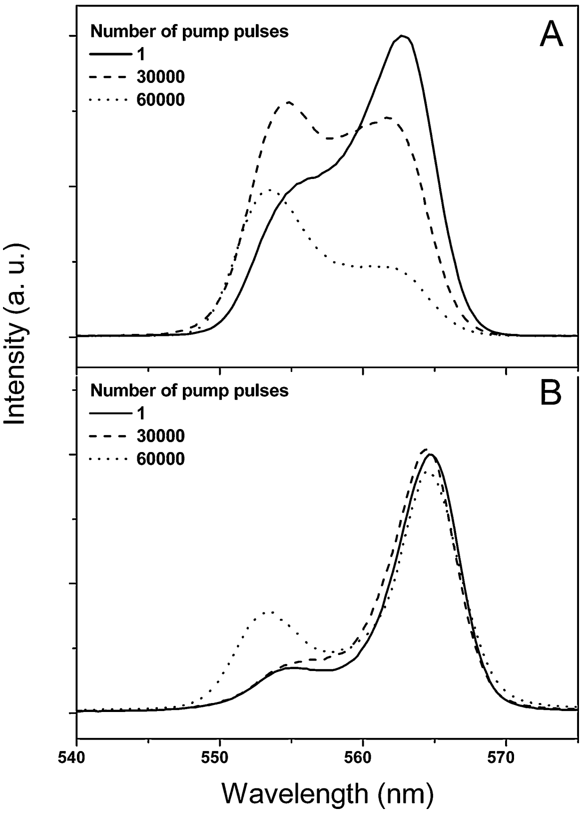

**FIGURE 10** Spectra of the laser emission for **A** P3Ac/COP(MMA–TFMA 7:3), and **B** TERP[P3MA–(MMA–TFMA 7:3)], after the indicated number of pump pulses in the same position of the sample

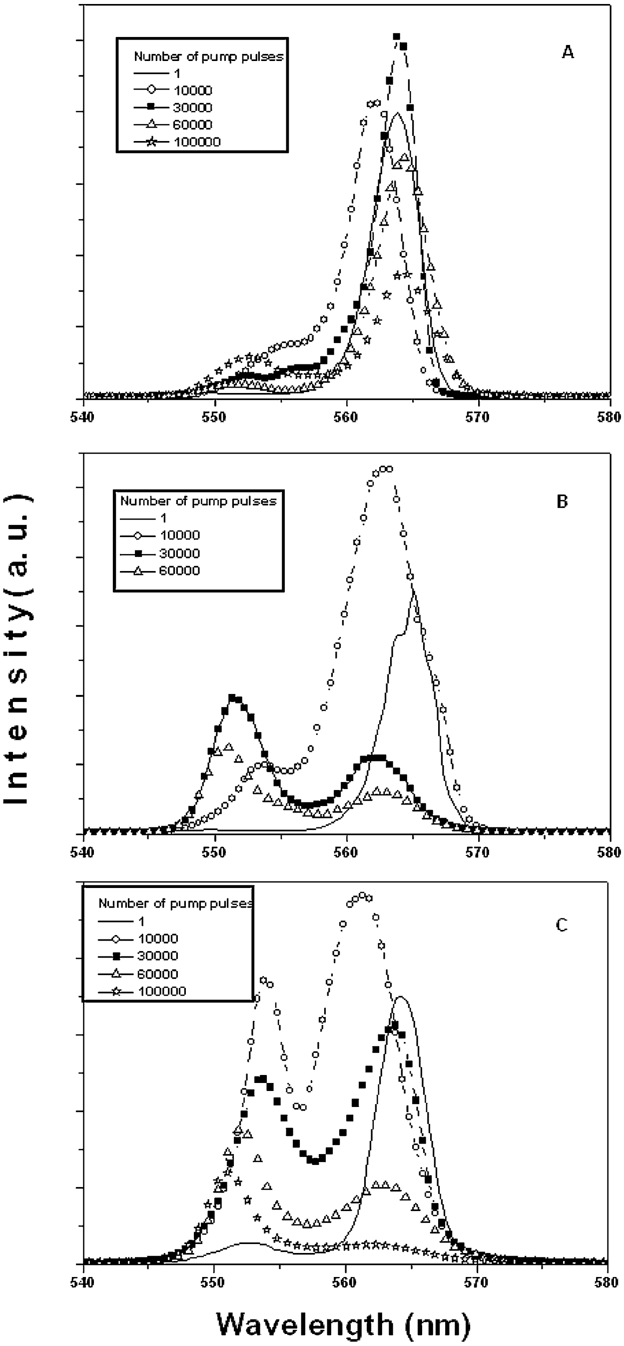

**FIGURE 11** Spectra of the laser emission for **A** TERP[P10MA–(MMA–PETRA 98:2)], **B** TERP[P10MA–(MMA–PETRA 90:10)], and **C** TERP[P10MA–(MMA–PETRA 80:20)], after the indicated number of pump pulses in the same position of the sample

the sample. At higher ratios of PETRA in the matrix (Fig. 11B and C) the second peak becomes more conspicuous and, as the number of pump pulses increases, ends being higher than the initial main lasing peak. In a matrix with P10MA dye copolymerized with MMA, with no PETRA, a similar second peak began to appear in the spectrum of the laser emission only after 300 000 pump pulses in the same position of the sample.

The data in Table 4 for the evolution of the laser output with the number of pump pulses correspond to the initial peak of the laser emission. Figure 12 shows the evolution of the intensity of the laser output with the number of pump pulses at the two peak wavelengths, i.e. at 563 and 551 nm for material TERP[P10MA–(MMA–PETRA 90:10)]. Initially, the laser emission at 563 nm drops while the emission at 551 nm increases steadily with an apparently correlated behaviour. After about 15 000 pump pulses the second emission was well established and from this point on both emissions evolved independently.

The above behaviour could be attributed to the formation of another laser emitting dye which we speculate could be formed by a scission reaction at position 8, which produces the separation of the alkyl radical group and the entrance of a hydrogen radical from the medium, giving rise to the PM567 analogue containing the same substituents at positions 1–3 and 5–7, but without substituent at position 8, herein denoted 8-H-PM. This speculation is based on two experimental facts: (1) dye 8-H-PM was found as a byproduct (traces) in the last step of the synthesis of all the analogues of PM567 studied herein [31], i.e. 8-H-PM appears from said analogues; and (2) a solid polymeric material formed with this synthetic 8-H-PM $0.5 \times 10^{-3}$ M in PMMA gave rise to laser emission with a peak at 554 nm, i.e. in the same region where the second laser peak appears in all checked polymeric samples. The intensity of this laser emission decreased with the number of pump pulses, but the lasing wavelength remained centred in the same region: after 30 000 pump pulses the emission dropped by 70% and the peak wavelength was 552 nm, the small shift being due to the decrease in dye concentration as a result of dye degradation. No second peak appeared now, indicating

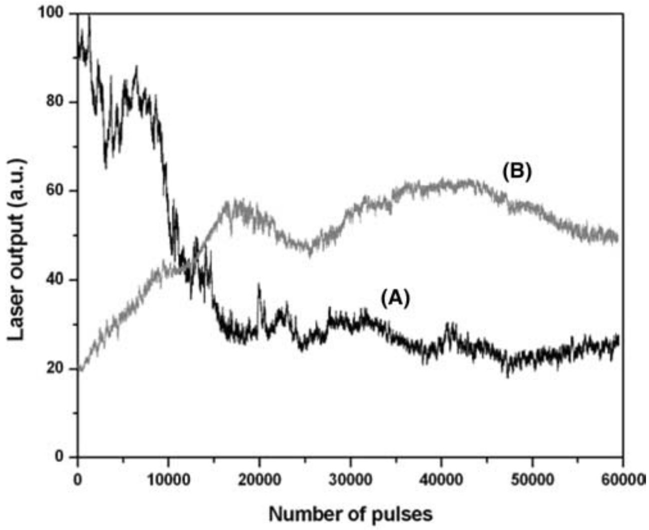

**FIGURE 12** Evolution of the laser output with the number of pump pulses at the two peak wavelengths of **A** 563 nm and **B** 551 nm for material TERP[P10MA–(MMA–PETRA 90:10)]

that the degradation now affects the chromophore core of compound 8-H-PM, leading to non-fluorescent products.

Further work directed to the unequivocal identification of the laser-generated dye was unsuccessful, likely because the absorption and fluorescence spectra of 8-H-PM, both in liquid solution and in polymeric matrices, are very similar to those in the same media of the PM567 analogues studied herein, with peak maxima differing by only a few nm. No changes were observed in the absorption and fluorescence spectral shapes in solid polymeric samples (1-cm-diameter disks) containing any of these analogues, after laser irradiation with the same number of pulses that resulted in the appearance of a distinct second peak in the laser emission from the laser rods. When the disks were irradiated under the same conditions as the laser rods, the small size of the irradiated surface ($10 \times 0.3\,\mathrm{mm}^2$) precludes the recording of the absorption and fluorescence spectra. When a wider area, of up to $10 \times 5\,\mathrm{mm}^2$, was irradiated, the pumping laser fluence was necessarily lower, which should result in the formation of a lower amount of the laser-generated product. In these conditions, even after increasing the number of pump pulses, we were not able to observe changes in the absorption and fluorescence spectra. On the other hand, the second laser peak did not appear when methanol solutions (0.25 mL) of the PM567 analogues were laser irradiated, even after $2 \times 10^6$ pump pulses, obviously as a result of the high volume involved and the small irradiated surface.

### 3.5 *Narrow-line-width operation*

It is well known that one of the most important features of dye lasers is their tunability, with narrow-line-width tuning ranges of tens of nanometres achieved with a single dye when a wavelength-selective resonator is utilized. Thus, the complete characterization of the herein studied dyes incorporated into solid matrices requires an assessment of their individual tuning capabilities.

It is seen from Tables 1, 2, 5, and 7 that dyes with 8-polymethylene chains with 3, 5, and 10 methylenes emit broad-line-width laser radiation in a simple plane-plane non-tunable resonator with peak wavelength in the range 560–570 nm, whereas the emission from dyes P1 (Tables 4 and 6) is red shifted to the range 589–594 nm. Thus, we chose dyes of each group to assess their tuning capability and to determine if, with just a couple of dyes in a proper tuning resonator, it would be possible to cover a wavelength region from the green to the red.

When a number of matrices incorporating covalently bound P1MA and P10MA dyes were placed in a grazing-incidence grating cavity in Shoshan configuration (Fig. 4), tunable laser emission with line width of the order of $0.15\,\mathrm{cm}^{-1}$ and efficiency of the order of 3% was obtained. Tuning ranges of up to 40 nm were observed (Table 8). By using just two materials, COP(P10MA–MMA) and TERP[P1MA–(MMA–PETRA 95:5)], the

| Material | $\lambda_{max}$ (nm) | $\Delta\lambda$ (nm) | Eff (%) | Laser output$^{b}$ | |
|---|---|---|---|---|---|
| | | | | 1 Hz $I_{10\,000}$ (%) | 10 Hz $I_{30\,000}$ (%) |
| PMMA | 562 | 7 | 12 | 70$^{c}$ | 16$^{d}$ |
| COP(MMA–HEMA 7:3)$^{c}$ | 561 | 5 | 9 | 70 | |
| COP(MMA–TFMA 7:3)$^{c}$ | 563 | 6 | 30 | 60 | |
| COP(MMA–EGDMA 95:5)$^{e}$ | 566 | 5 | 10 | | 11$^{f}$ |
| COP(MMA–TMPTMA 95:5)$^{e}$ | 564 | 5 | 19 | | 20$^{g}$ |
| COP(MMA–PETA 95:5) | 568 | 5 | 21 | | 12 |
| COP(MMA–PETRA 95:5) | 564 | 6 | 18 | | 80 |

Dye concentration: $1.5 \times 10^{-3}$ M

[a] As defined in Table 1

[b] As defined in Table 1, at the stated pump repetition rates

[c] Data from Ref. [16]

[d] Data from Ref. [28]

[e] Data from Ref. [17]

[f] After 17 000 pump pulses

[g] After 18 000 pump pulses

**TABLE 7** Laser parameters[a] for dye PM567 dissolved in homopolymer PMMA and in linear and cross-linked copolymers (COP)

| Material | Tuning range (nm) |
|---|---|
| TERP[P1MA–(MMA–PETRA 95:5)] | 576–616 |
| TERP[P1MA–(MMA–TMPTMA 95:55)] | 585–606 |
| COP(P10MA–MMA) | 552–586 |
| TERP[P10MA–(MMA–PETRA 98:2)] | 554–582 |
| TERP[P10MA–(MMA–PETRA 80:20)] | 556–576 |

Dye concentration: $1.5 \times 10^{-3}$ M

**TABLE 8** Tuning range of covalently bound P1MA and P10MA monomeric dyes in different polymeric formulations

region 552–616 nm can be continuously covered with narrow-line-width laser radiation.

The evolution of the narrow-line-width tunable operation with the number of laser shots was studied by pumping material TERP[P10MA–(MMA–PETRA 80:20)] at 10-Hz repetition rate and determining the range of tunability of the narrow-line emission and the increase of the ASE (amplified spontaneous emission) background after every 10 000 pump pulses in the same position of the sample. The initial tuning range was 28 nm (from 554 to 582 nm) and the ASE content was 2% of the total laser emission. After 30 000 pump pulses, the tuning range decreased to 11 nm (from 559 to 570 nm), the peak intensity of the narrow-line emission was 6% of the initial intensity, and the ASE content was 52% of the total laser emission. After 60 000 pump pulses, the tuning range remained at 11 nm but the peak intensity of the narrow-line emission was just 1% of the initial intensity and the ASE content increased to 71% of the total laser emission. The second-peak formation discussed in Sect. 3.4 was not observed to influence the tunability range. Probably, the increased losses with the number of pump pulses, which result in the reduction of the tuning range, decrease the gain in the region of the second peak below the lasing threshold for narrow-line-width emission.

### 3.6 *Comparison with previous results*

Results obtained with reference dye PM567 in the homopolymer PMMA and in linear and cross-linked copolymers are collected in Table 7. When these results are compared with those collected in Tables 1 and 3, it is seen that the lasing efficiencies obtained with the 8-substituted alkyl analogues of PM567 are much higher than those obtained with the dye PM567 in the same matrices, except for dye P3Ac in matrices containing TFMA.

The stability obtained with linear copolymers containing the model dyes (dissolved) or the monomeric dyes (covalently bound) was in all cases much higher than that obtained with PM567 in the same materials: comparison of data in Tables 1 and 7 shows that for materials with HEMA and TFMA the laser output of dissolved P*n*Ac and covalently bound P*n*MA dyes after 30 000 pump pulses at 10-Hz repetition rate is in most cases higher than the laser output from PM567 dye in the same materials after just 10 000 pump pulses at the less demanding 1-Hz repetition rate. When the dyes were incorporated into cross-linked copolymers, materials are always found in which both dissolved P*n*Ac and covalently bound P*n*MA ($n = 3, 5, 10$) dyes exhibited higher photostability than the highest one reached with PM567 (compare Tables 3 and 7).

The results reported in this work compare well, or even improve, previous results obtained by other authors on dipyrromethene dyes incorporated into polymeric matrices. Lasing efficiencies of up to 71% have been reported for PM567 dissolved in PMMA incorporating perylene additives [14]. With PM567 dissolved in a modified and non-well-defined acrylic ‘plastic’, efficiencies as high as 77% were obtained, which increased to 85% when the dye was PM570 [35]. It should be pointed out that these results are not directly comparable with those reported herein because they were obtained under longitudinal pumping and with the oscillator cavity optimized, whereas our studies have been performed under transversal pumping and with a non-optimized laser cavity. In the only previous study of dipyrromethene dyes incorporated into polymeric matrices where a transversal pumping configuration was utilized [36], the lasing efficiency found was 49%, not much higher than those obtained with our modified dipyrromethene·$BF_2$ dyes, and this higher efficiency was obtained by using a zigzag optical configuration that increases the optical path of the radiation inside the gain medium.

Direct comparison of our stability results with those obtained by other authors is a difficult task because of the substantial differences in experimental conditions, such as repetition rate or pumping configuration, which can strongly affect the longevity of the solid samples. In order to facilitate comparisons in a way independent of the experimental setup, Rahn and King [37] introduced a normalized photostability defined as the accumulated pump energy absorbed by the system per mole of dye molecules before the output energy falls to one-half of its initial value. Its units are gigajoules per mole (GJ/mol). In our case, we estimate for TERP(P5MA–MMA–PETRA) an accumulated absorbed pump energy per mole of dye molecules of 180 GJ/mol after 95 000 pump pulses at 10-Hz repetition rate, where the laser emission still remained at 88% of its initial value (Table 5). Similar or higher values were obtained with other terpolymers, such as TERP[P3MA–(MMA–TMPTMA 95:5)] or TERP[P10MA–(MMA–TMPTMA 99:1)]. The best previous results from other authors on polymeric solid-state dye lasers based on dipyrromethene dyes were obtained with PM567 incorporated into a matrix of PMMA in the presence of DABCO (1,4-diazobicyclo[2, 2, 2]octane), in which case the laser output decreased by 50% after an accumulated absorbed pump energy per mole of dye molecules of 190 GJ/mol at 10-Hz repetition rate or 270 GJ/mol at 2-Hz repetition rate [14, 18]. By mixing PM567 with coumarin 540, Ahmad et al. [38] obtained a normalized photostability of 350 GJ/mol in dye-doped PMMA samples pumped at 10 Hz with 532-nm pulses at a fluence of 1.0 J/cm$^2$.

## 4 Conclusions

In this paper we report efficient and highly photostable laser operation from modified dipyrromethene·$BF_2$ dye analogues of the commercial dye PM567 when incorporated (dissolved or copolymerized) into polymeric matrices prepared with linear or cross-linked copolymers with different degrees of functionalization. Under transversal pumping at 534 nm, lasing efficiencies of up to 40% were obtained, whereas the maximum efficiency obtained with dye PM567 in the same materials and under the same experimental conditions was 30%. Although good photostabilities were obtained with dyes incorporated into some of the linear copolymers, the highest photostabilities were reached in cross-linked materials with the chromophores covalently linked to the polymer chains, with the laser output remaining stable or dropping by less than 15% after 100 000 pump pulses at the same position of the sample at 10-Hz repetition rate in some of them. In all cases, to obtain high photostability it is required that the cross-linking monomer has at least three reactive double bonds. When the solid-state dye lasers developed in this work were incorporated into a wavelength-selective resonator, narrow-line-width laser operation with tuning ranges of up to 40 nm were obtained. By using just two dyes, it was possible to cover the region from 552 to 616 nm with continuous tunable narrow-line-width laser radiation.

The results reported in this work show that appropriate modifications in the dipyrromethene·$BF_2$ dyes and in their environment can yield materials that lase efficiently and with remarkable photostability, making these solid-state dye lasers fully competitive with their liquid counterparts.

The materials described in this work and their utilization in solid-state dye lasers are covered by Spanish Patent No. 9901540 filed on 9 July 1999. A part of the results reported here was presented at the conference Photonics Europe 2004.

**ACKNOWLEDGEMENTS** This work was supported by Project MAT2000-1361-C04-01 of the Spanish CICYT. C. Gómez and M. Álvarez thank Comunidad de Madrid and Ministerio de Ciencia y Tecnología for postdoctoral and predoctoral scholarships, respectively.

## REFERENCES

1 A. Costela, I. García-Moreno, R. Sastre, in *Handbook of Advanced Electronic and Photonic Materials and Devices*, vol. 7, ed. by H.S. Nalwa (Academic, San Diego, 2001), pp. 161–208
2 R. Sastre, A. Costela, Adv. Mater. **7**, 198 (1995)
3 T.G. Pavlopoulos, M. Sha, J.H. Boyer, Appl. Opt. **27**, 4998 (1988)
4 T.G. Pavlopoulos, M. Sha, J.H. Boyer, Opt. Commun. **70**, 425 (1989)
5 M. Sha, K. Thangaraj, M.-L. Soong, L.T. Wolford, J.H. Boyer, I.R. Politzer, T.G. Pavlopoulos, Heteroatom Chem. **1**, 389 (1990)
6 T.G. Pavlopoulos, J.H. Boyer, M. Sha, K. Thangaraj, M.-L. Soong, Appl. Opt. **29**, 3885 (1990)
7 J.H. Boyer, A. Haag, M.-L. Soong, K. Thangaraj, T.G. Pavlopoulos, Appl. Opt. **30**, 3788 (1991)
8 T.G. Pavlopoulos, J.H. Boyer, K. Thangaraj, G. Sathyamoorthi, M.P. Sha, M.-L. Soong, Appl. Opt. **31**, 7089 (1991)
9 S.C. Guggenheimer, J.H. Boyer, K. Thangaraj, M.-L. Soong, T.G. Pavlopoulos, Appl. Opt. **32**, 3942 (1993)
10 J.H. Boyer, A. Haag, G. Sathyamoorthi, M.-L. Soong, K. Thangaraj, T.G. Pavlopoulos, Heteroatom Chem. **4**, 39 (1993)
11 M.P. O'Neil, Opt. Lett. **18**, 37 (1993)
12 W.P. Partridge, Jr., N.M. Laurendeau, C.C. Johnson, R.N. Steppel, Opt. Lett. **19**, 1639 (1994)
13 Y. Assor, Z. Burshtein, S. Rosenwaks, Appl. Opt. **37**, 4914 (1988)
14 M. Ahmad, M.D. Rahn, T.A. King, Appl. Opt. **38**, 6337 (1999)
15 E. Yariv, R. Reisfeld, Opt. Mater. **13**, 49 (1999)
16 A. Costela, I. García-Moreno, J. Barroso, R. Sastre, Appl. Phys. B **70**, 367 (2000)
17 A. Costela, I. García-Moreno, C. Gómez, O. García, R. Sastre, J. Appl. Phys. **90**, 3159 (2001)
18 M. Ahmad, T.A. King, D. Ko, B.H. Cha, J. Lee, Opt. Commun. **203**, 327 (2002)
19 Y. Yang, G. Qian, Z. Wang, M. Wang, Opt. Commun. **204**, 277 (2002)
20 Q.Y. Zhang, W.X. Que, S. Buddhudu, K. Pita, J. Phys. Chem. Solids **63**, 1723 (2002)
21 A. Costela, I. García-Moreno, C. Gómez, O. García, R. Sastre, Chem. Phys. Lett. **369**, 656 (2003)
22 T.H. Nhung, M. Canva, T.T.A. Dao, F. Chaput, A. Brun, N.D. Hung, J.P. Boilot, Appl. Opt. **42**, 2213 (2003)
23 Y. Yang, M. Wang, G. Qian, Z. Wang, X. Fan, Opt. Mater. **24**, 621 (2004)
24 M.D. Rahn, T.A. King, A.A. Gorman, I. Hamblett, Appl. Opt. **36**, 5862 (1997)
25 T. López Arbeloa, F. López Arbeloa, I. López Arbeloa, I. García-Moreno, A. Costela, R. Sastre, F. Amat-Guerri, Chem. Phys. Lett. **299**, 315 (1999)
26 A. Costela, I. García-Moreno, C. Gómez, F. Amat-Guerri, R. Sastre, Appl. Phys. Lett. **79**, 305 (2001)
27 F. Liang, H. Zeng, Z. Sun, Y. Yuan, Z. Yao, Z. Xu, J. Opt. Soc. Am. B **18**, 1841 (2001)
28 A. Costela, I. García-Moreno, C. Gómez, F. Amat-Guerri, M. Liras, R. Sastre, Appl. Phys. B **76**, 365 (2003)
29 T.G. Pavlopoulos, Prog. Quantum Electron. **26**, 193 (2002)
30 A. Costela, I. García-Moreno, C. Gómez, R. Sastre, F. Amat-Guerri, M. Liras, F. López Arbeloa, J. Bañuelos Prieto, I. López Arbeloa, J. Phys. Chem. A **106**, 7736 (2002)
31 F. Amat-Guerri, M. Liras, M.L. Carrascoso, R. Sastre, Photochem. Photobiol. **77**, 577 (2003)
32 F. López Arbeloa, J. Bañuelos, I. López Arbeloa, A. Costela, I. García-Moreno, C. Gómez, F. Amat-Guerri, M. Liras, R. Sastre, Photochem. Photobiol. **78**, 30 (2003)
33 M. Rodríguez, A. Costela, I. García-Moreno, F. Florido, J.M. Figuera, R. Sastre, Meas. Sci. Technol. **9**, 971 (1995)
34 I. Shoshan, N.N. Danon, U.P. Oppenheim, J. Appl. Phys. **48**, 4495 (1977)
35 R.E. Hermes, T.H. Allik, S. Chandra, J.A. Hutchinson, Appl. Phys. Lett. **63**, 877 (1993)
36 A. Mandl, A. Zavriyev, D.E. Klimek, IEEE J. Quantum Electron. **32**, 1723 (1996)
37 M.D. Rahn, T.A. King, Appl. Opt. **34**, 8260 (1995)
38 M. Ahmad, T.A. King, D. Ko, B.H. Cha, J. Lee, Opt. Laser Technol. **34**, 445 (2002)